Supporting Information

Mo^{IV}_3…$[O_8Mo_4]_3$ Lewis acid-base cluster pairs: Highly efficient and stable Lewis catalysis fields frustrated in crystalline nanoclusters

Fang Yu,[ab] Benlong Luo,[a] Ruili Sang,[a] Li Xu*[a]

[a]State Key Laboratory of Structural Chemistry, Fujian Institute of Research on the Structure of Matter, Chinese Academy of Sciences, Fuzhou, Fujian, 350002.

[b]University of Chinese Academy of Sciences, Beijing, 100049, China.

xli@fjirsm.ac.cn

1. Experimental Section

1.1 Methods and Materials

All chemicals were obtained from commercial sources and used without further purification. Elemental analyses (C, H and N) were performed using a vario MICRO elemental analyzer. ICP-OES (Inductively Coupled Plasma Optical Emission Spectroscopy) analyses (Al, V, Mo) were carried on Ultima 2. IR spectra were recorded with a Magna 750 FTIR spectrometer photometer as KBr pellets in the 4000–400 cm^{-1} region. Mass spectroscopic measurements were carried out on a Bruker-Impact II-UHR-TOF. The X-ray photoelectron spectroscopy (XPS) measurements were carried out on a ESCALAB 250Xi spectrometer equipped with an Al K_α X-ray source. The intensity data were collected on a Bruker D8-venture diffractometer with graphite-monochromated MoKα radiation (λ= 0.71073 Å). All absorption corrections were performed using multiscan. The structures were solved by direct methods and refined by full-matrix least-squares on F^2 with the SHELXTL-2016 program package.

1.2 Synthesis

$[Mo^{IV}_3O_2(O_2CCH_3)_6(H_2O)_3]ZnCl_4{\cdot}8H_2O$ was prepared according to the published procedure.[19]

$\{H_{10}[Al_2@Mo_{30}O_{80}py_{12}]\}_3{\cdot}10C_5H_5N{\cdot}17H_2O$ (**1**) (H_{30}[**1a**][**1b**][**1c**]$\cdot10C_5H_5N\cdot17H_2O$).

$[Mo_3O_2(O_2CCH_3)_6(H_2O)_3]ZnCl_4{\cdot}8H_2O$ (0.1 g, 0.1 mmol), $AlCl_3$ (0.05g, 0.04 mmol) was added into a mixture of H_2O (3 mL) and pyridine (7 mL). The filtrate was sealed in a 20 mL teflonlined stainless-steel reactor and heated at 148℃ for two days. The reactor was cooled to room temperature at a rate of 0.5K/min to produce black crystals of **1** (>20% yield based on Mo). IR (KBr): 1609m (py),1450m (py), 972s (Mo^{VI}=O), 860w (Mo^{VI}-O-Mo), 752s [$Mo^{IV}_3O_4$]. MS(m/z, CH_3CN)(simulated): $[Al_2@Mo_{30}O_{80}py_9(H_2O)_3H_8]$, 2493.1118 (2493.1050); $[Mo_{30}Al_2O_{80}py_7(H_2O)_5(CH_3CN)_2H_8]^{2-}$, 2473.1058 (2473.0998); $[Mo_{30}Al_2O_{80}py_8(H_2O)_5(CH_3CN)_2H_8]^{2-}$, 2512.6252 (2512.6196); MS(m/z, pyridine)(simulated): $[Mo_{30}Al_2O_{80}py_9(H_2O)_3H_8]^{2-}$, 2493.1079 (2493.1036). monoclinic, *C*2, a = 57.6292(15), b = 16.9770(5), c = 48.8318(13) Å, V = 43182(2) $Å^3$, Z = 4, R1/wR2 =9.35/30.28% for the observed data (I ≥2σ(I)), R1/wR2 = 9.68/30.61% for all data; CCDC-2004047.

$H_{16}[V_2@Mo_{30}O_{84}py_{12}][V_3Mo_{12}O_{42}]_3{\cdot}10H_2O{\cdot}3py$ (**2**) (H_{16}[**2a**][**2b**]$_3\cdot10H_2O\cdot3$py).

$[Mo_3O_2(O_2CCH_3)_6(H_2O)_3]ZnCl_4{\cdot}8H_2O$ (0.1 g, 0.1 mmol), $VO(acac)_2$, (0.01g, 0.04 mmol) was added into a mixture of H_2O (1 mL), DMF (0.5mL) and pyridine (8 mL). The resulting mixture was sealed in a 20 mL teflonlined stainless-steel reactor and heated at 140℃ for two days. The reactor was cooled to room temperature at a rate of 1K/h to produce the black crystals of **2**. ICP analyses: Mo, 48.30%, V, 4.24%, the ratio of atomic number, Mo/V = 6.05; calcd. Mo/V = 66/11 = 6. IR (KBr): 3484m (H_2O), 3071m (py), 1607m (py), 1448m (py), 947m (M^{I}=O), 872vs (M-O-Mo), 756s ([$Mo^{IV}_3O_4$]). cubic, *F*$m\bar{3}$m, a = 42.3973(18) Å, V = 76211(9) $Å^3$, Z = 8, R1/wR2 =5.88/17.57% for the observed data (I ≥2σ(I)), R1/wR2 = 6.81/18.86% for all data; CCDC-2004115.

$H_{12}[Mo_2@Mo_{30}O_{84}py_{12}]{\cdot}[Ge_2Mo_{13}O_{41}(OH)_2]_3$ (**3**) (H_{12}[**3a**][**3b**]$_3$).

$[Mo_3O_2(O_2CCH_3)_6(H_2O)_3]ZnCl_4{\cdot}8H_2O$ (0.1 g, 0.1 mmol), GeO_2(0.0117 g, 0.112 mmol) and $HOCH_2CO_2H$ (0.012 g, 0.158 mmol) was added into a mixture of H_2O (2 mL), DMF (0.5mL) and pyridine (8 mL). The resulting mixture was sealed in a 20 mL teflonlined stainless-steel reactor and heated at 140℃ for two days. The reactor was cooled to room temperature at a rate of 1K/h to produce black crystals of **3**. cubic, *F*$m\bar{3}$m, a = 42.593(2) Å, V = 77270(11) $Å^3$, Z = 8, R1/wR2 =5.55/13.30% for the observed data (I ≥2σ(I)), R1/wR2 = 8.14/14.97% for all data; CCDC-2004116.

2. Structures

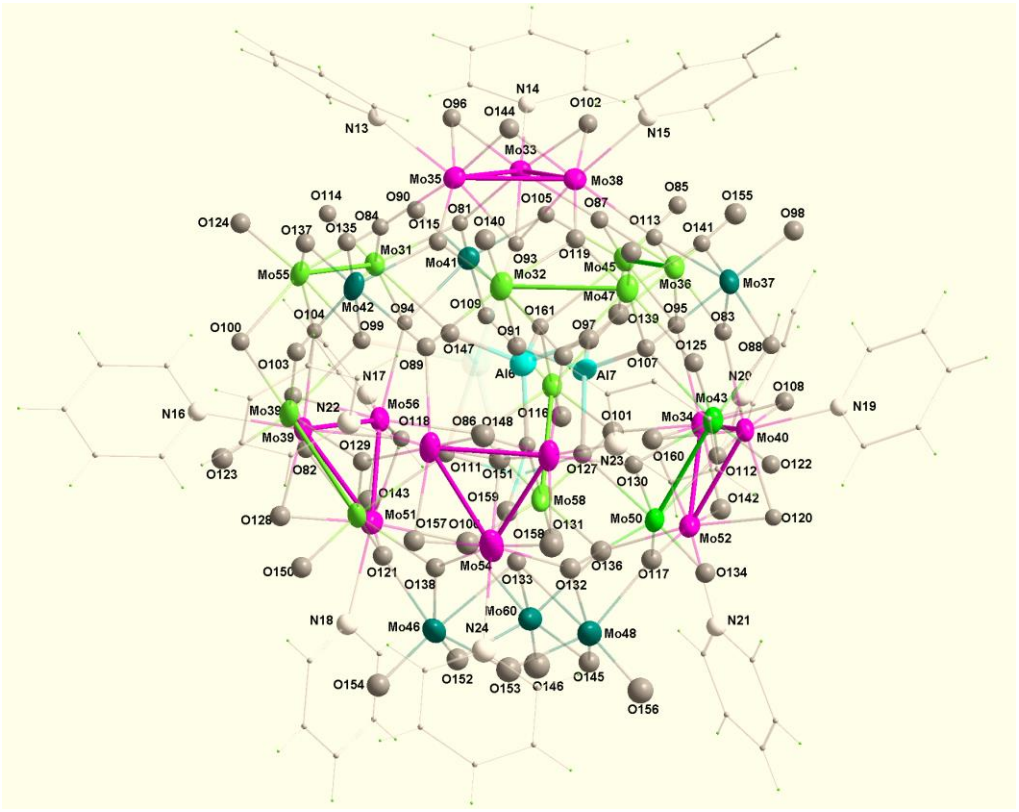

Fig. S1 Atomically labeled structure of $[H_4Al_2@Mo_{30}O_{80}py_{12}]^{6-}$ (**1a**) with 50% (Al), 30% (Mo) and 20% (O, N) probability thermal ellipsoids (Mo^{IV}, purple; Mo^{V}, green; Mo^{VI}, black green, Al^{3+}, aqua; O, N, grey).

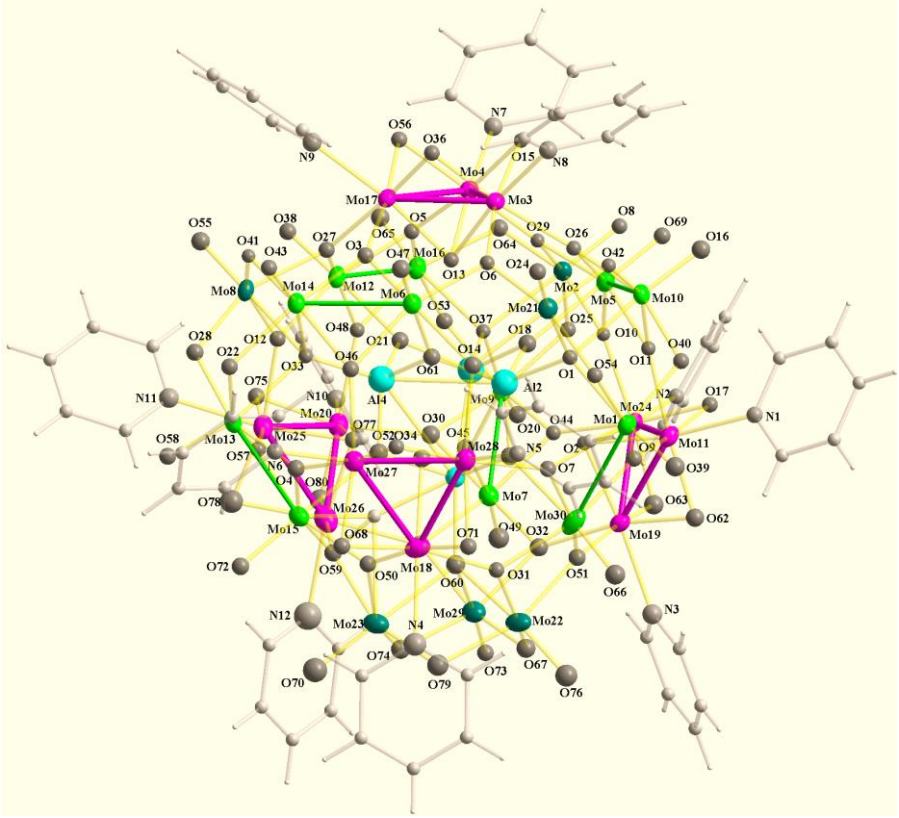

Fig. S2 Atomically labeled Structure of $[H_4Al_2@Mo_{30}O_{80}py_{12}]^{6-}$ (**1b**) with 50% (Al), 30% (Mo) and 20% (O, N) probability thermal ellipsoids (Mo^{IV}, purple; Mo^{V}, green; Mo^{VI}, black green, Al^{3+}, aqua; O, N, grey). Al•••Al, 2.902(1) Å.

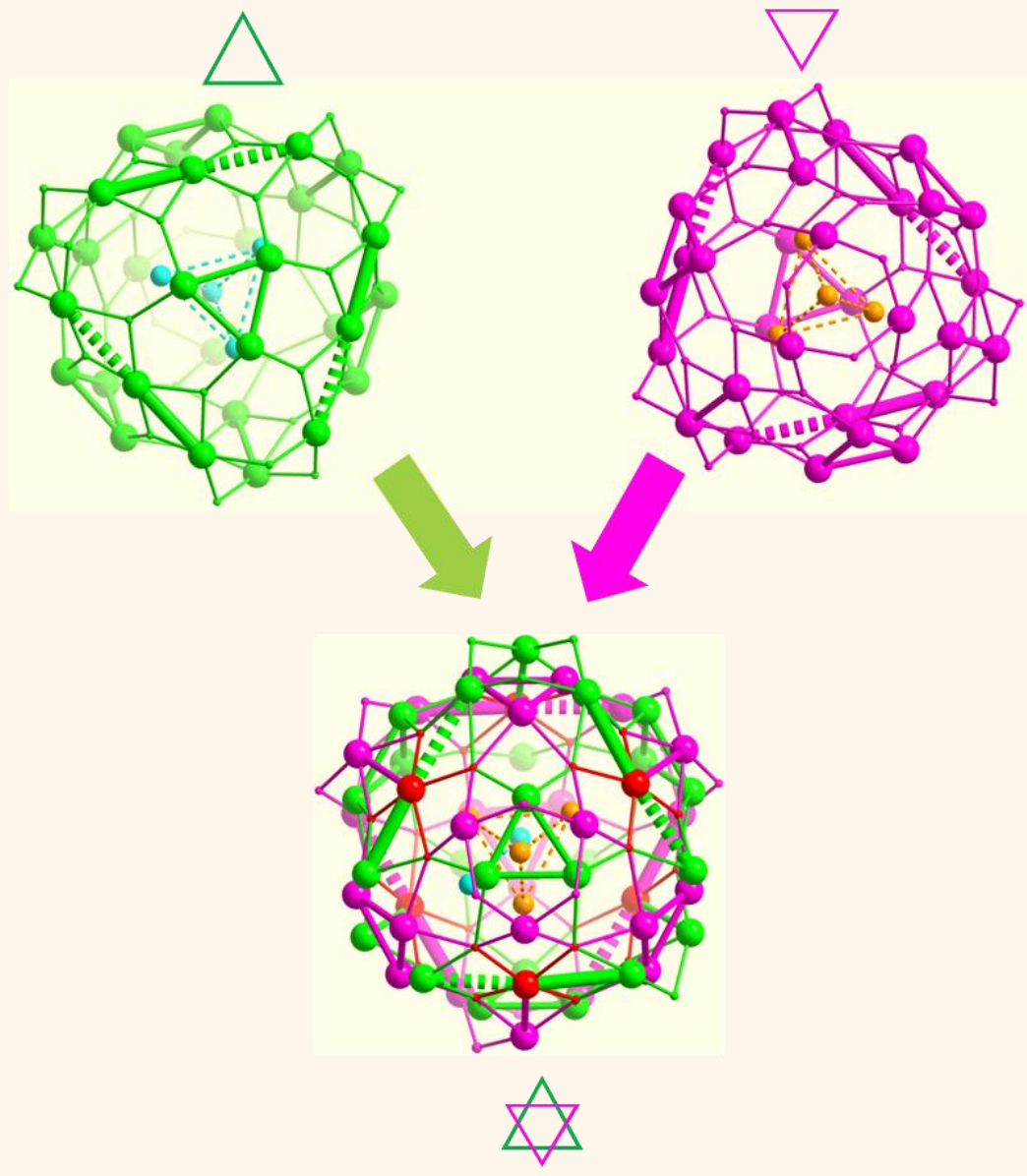

Fig. S3 Seriously disordered structure of $[Al_2@Mo_{30}O_{80}py_{12}]$ (**1c**) formed through a reverse alternative arrangement of **1a** and **1b**.

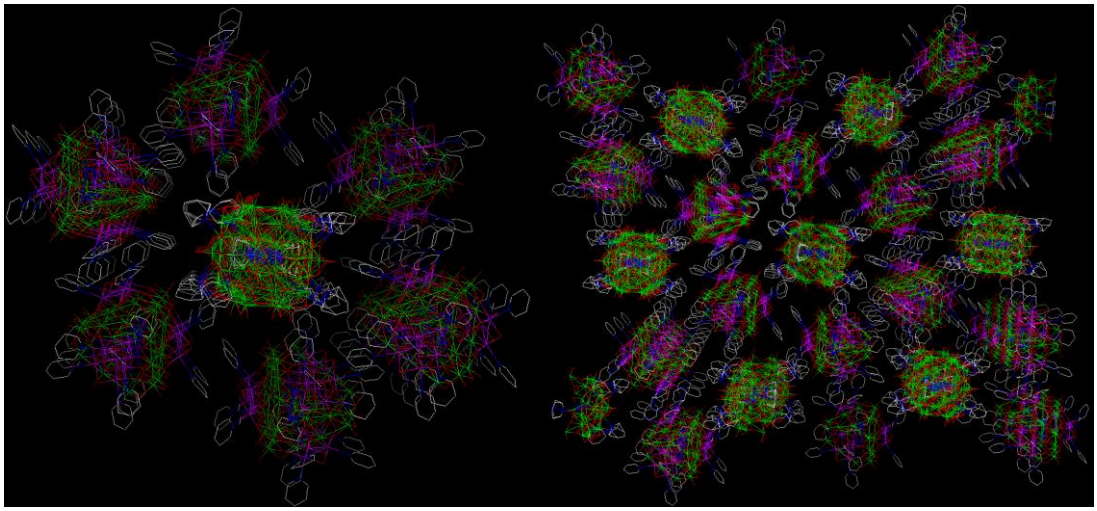

Fig. S4 Crystal pacing diagram of **1** showing neighboring arrangement of $[Mo^{IV}_3py_3](Mo^{IV}_3$, purple triangle).

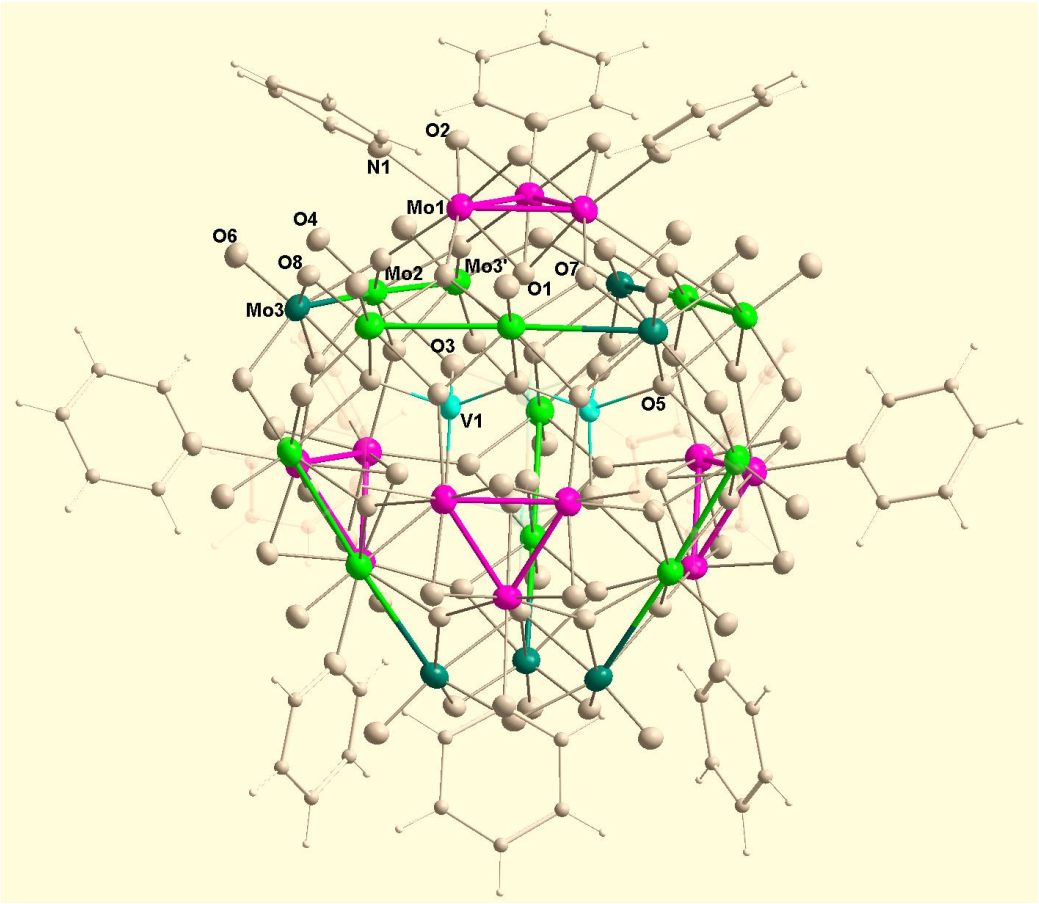

Fig. S5 Atomically labeled structure of $[V_2@Mo_{30}O_{80}py_{12}]$ (**2a**) with 30% (V, Mo) and 20% (O, N) probability thermal ellipsoids (Mo^{IV}, purple; V^{IV}, aqua; Mo^{V}, Mo^{VI}, green and black green, O, N, grey). Selected bond lengths: Mo1-Mo1, 2.492(2); Mo2-Mo3, 2.846 (2), V1•••V1', 2.779(2) Å.

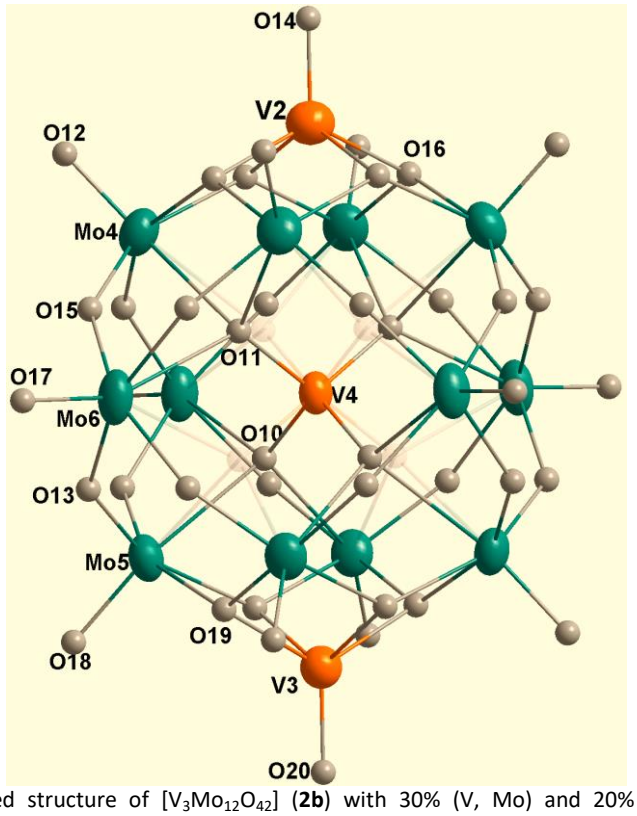

Fig. S6 Atomically labeled structure of $[V_3Mo_{12}O_{42}]$ (**2b**) with 30% (V, Mo) and 20% probability thermal ellipsoids (Mo^{VI}, black green, O, N, grey).

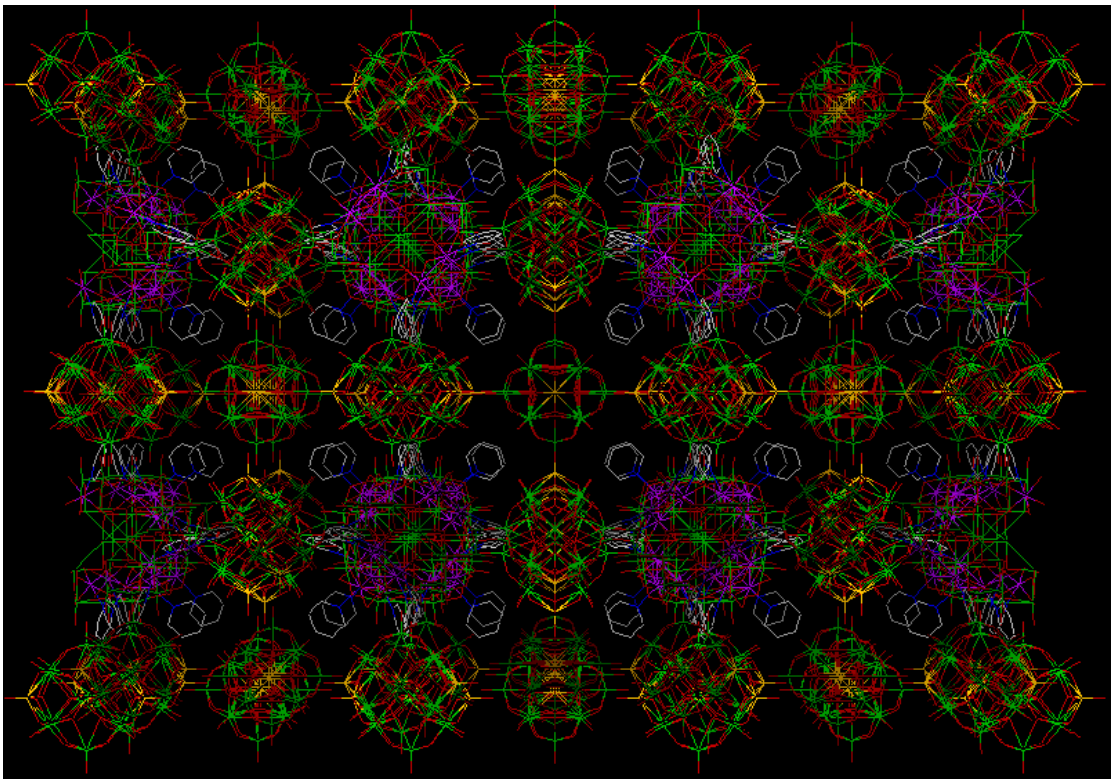

Fig. S7 Crystal packing diagram of **2** showing each **2a** and surrounding twelve **2b**.

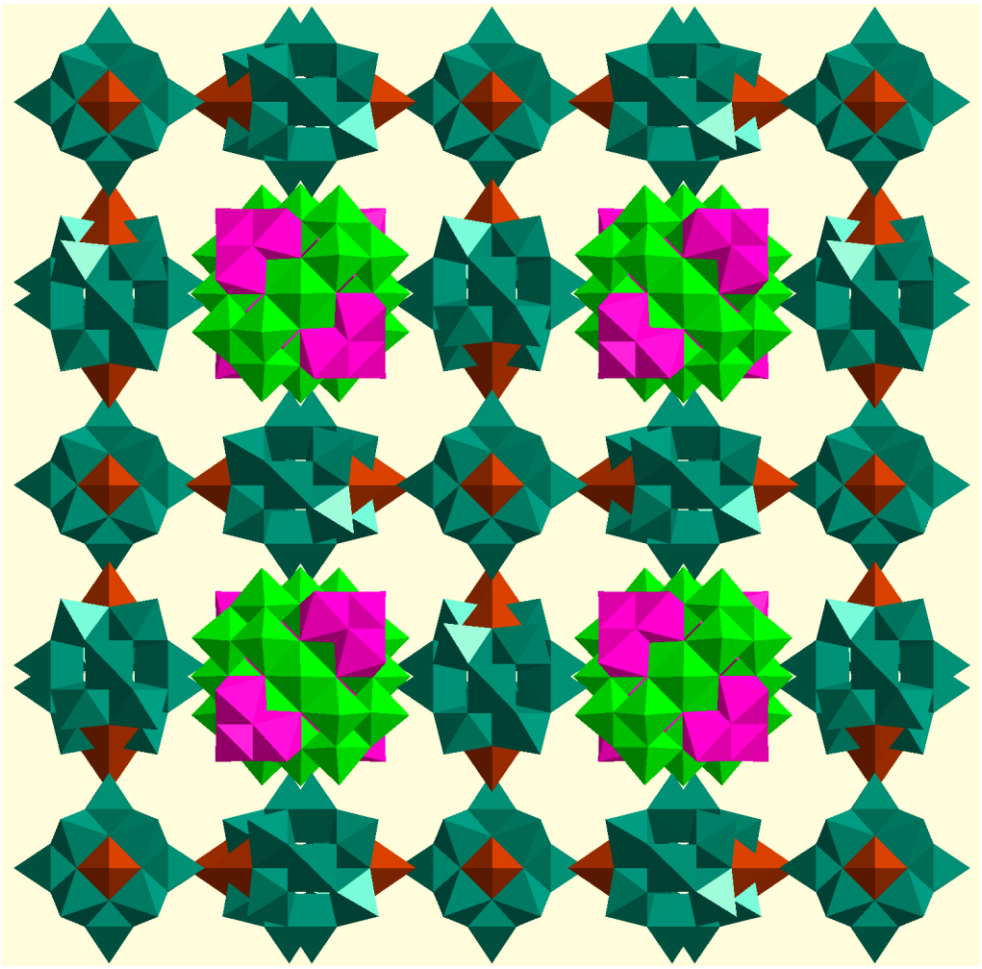

Fig. S8 Polyhedral presentation of crystal packing diagram of **2** showing each **2a** and surrounding twelve **2b**.

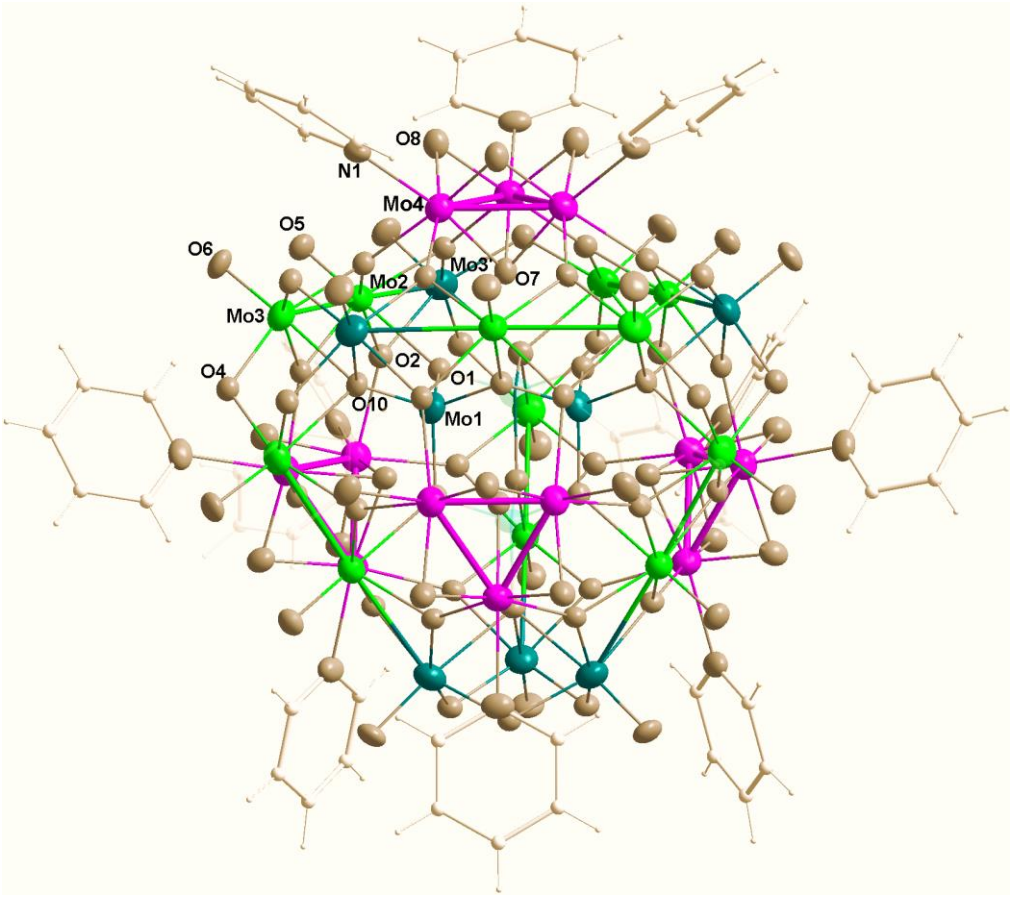

Fig. S9 Atomically labeled structure of $[Mo_2@Mo_{30}O_{80}py_{12}]$ (**3a**) with 30% (Mo) and 20% (O, N) probability thermal ellipsoids (Mo^{IV}, purple; Mo^{V}, Mo^{VI}, green and black green, O, N, grey). Selected bond lengths: Mo4-Mo4, 2.497(2); Mo2-Mo3, 2.8541 (15), Mo1•••Mo1', 2.942(7) Å.

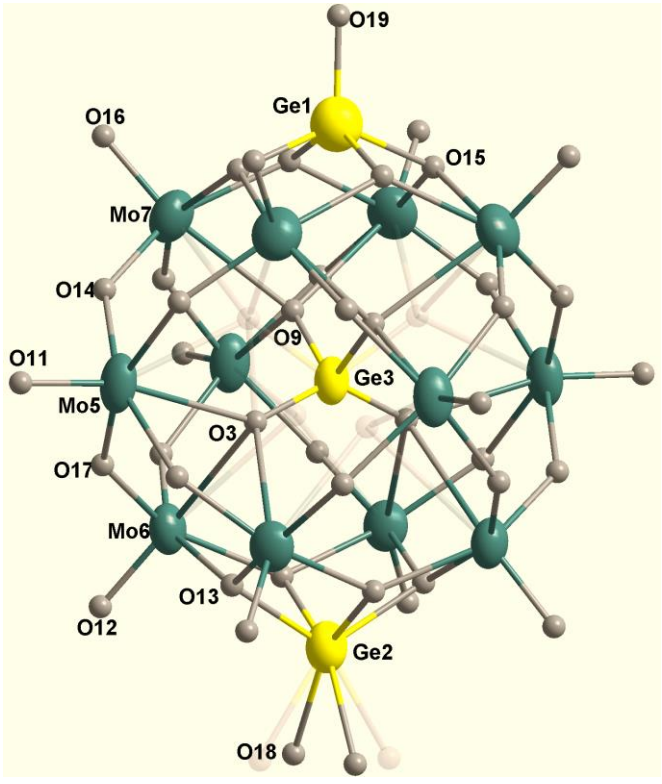

Fig. S10 Atomically labeled structure of $[Ge_3Mo_{12}O_{43}]$ (**3b**) with 30% (Ge, Mo) probability thermal ellipsoids (Ge^{IV}, yellow; Mo^{VI}, black green; O, grey).

3. XPS spectra

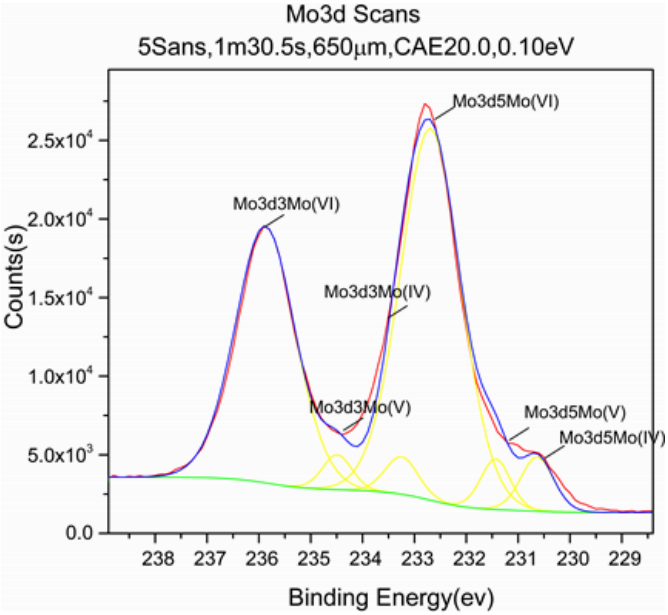

Fig. S11 XPS of **2**.

Binding energies of Mo 3d from the literatures [20, 22] and the binding energies of peaks used to assign species from the present measurements of **2** (C1S calibrated to 284.8ev for contrast).

A comparison of $Mo^{IV,V,VI}$ binding energies in **2** and related compounds

Oxidation state	Mo $3d_{5/2}$ (eV)	Mo $3d_{3/2}$ (eV)
Mo(IV)-$MoO(OH)_2$	230.2	233.4
Mo(V)-$MoCl_5$	230.9-231.1	234.3-235.4
Mo(VI)-$Na_2MoO_4{\cdot}2H_2O$	231.9-232.3	235-235.4
Mo(IV)-**2**	230.52	233.57
Mo(V)-**2**	231.21	234.26
Mo(VI)-**2**	232.74	235.89
Mo(IV)-**10** [22]	230.11	233.27
Mo(V)-**10** [22]	231.63	234.74
Mo(VI)-**10** [22]	232.11	235.46
Mo(IV)-**9** [20]	229.12	232.28
Mo(V)-**9** [20]	230.26	233.30
Mo(VI)-**9** [20]	231.14	234.20

$H_4[Mo^{IV}_6Mo^{V}_6Mo^{VI}_9O_{54}(OH)_4py_6]$ (**10**),[22] $Na[Mo^{IV}_{12}Mo^{V}_4Mo^{VI}_3O_{43}(OH)Py_{12}]$ (**9**) [20]

4. IR spectra

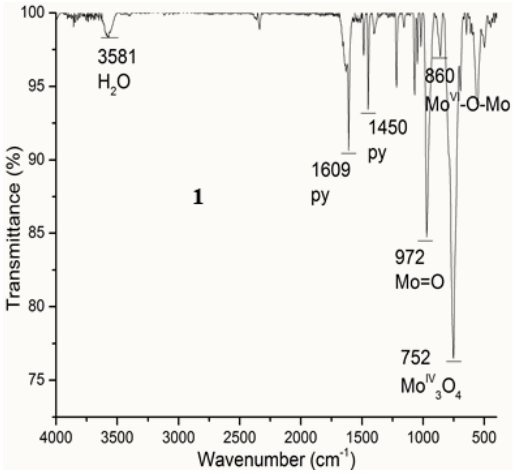

Fig. S12 IR spectrum of **1.**

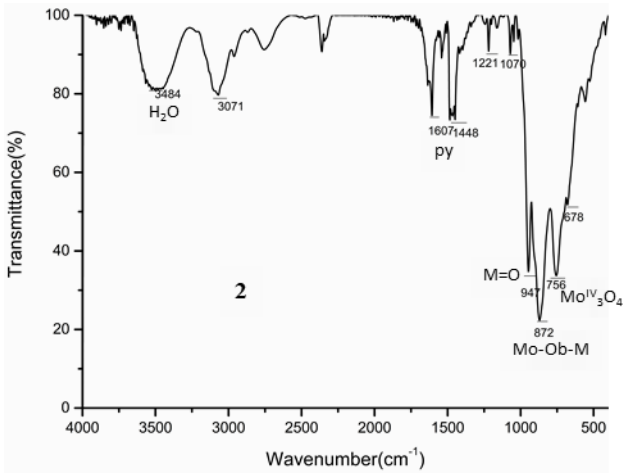

Fig. S13 IR spectra of **2.**

5. Characterization data of the isolated products.

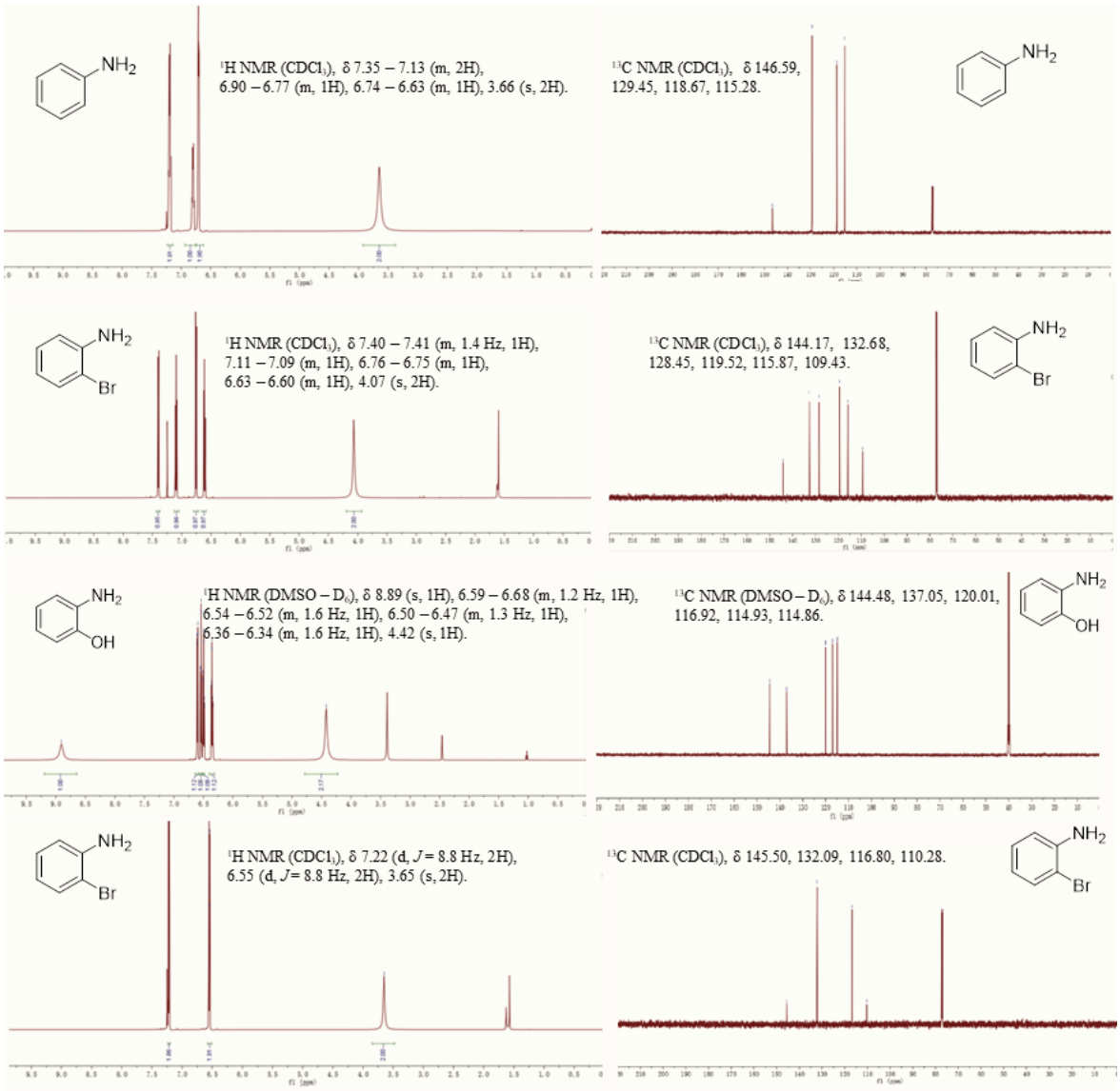

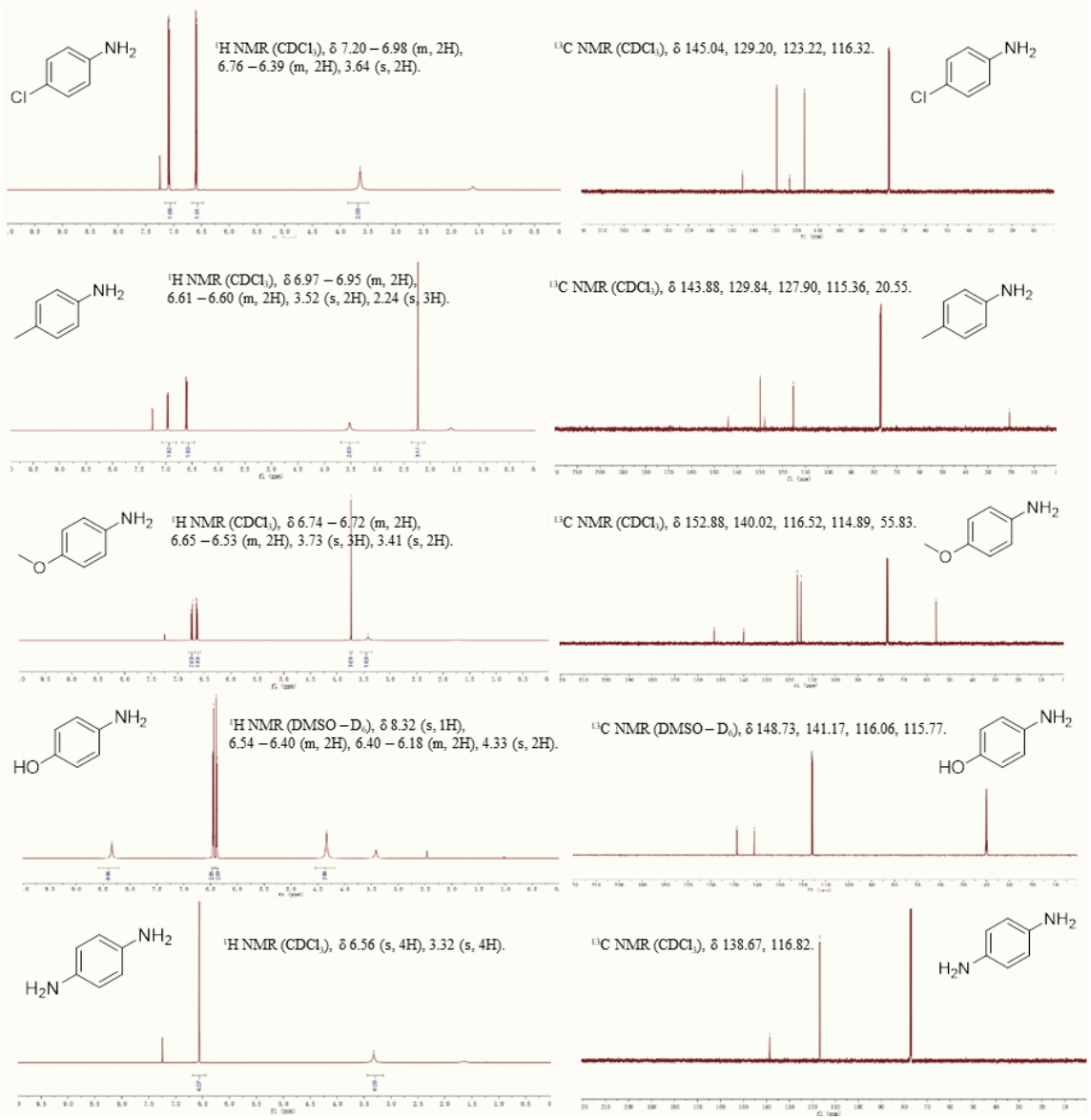

Fig. S14. ^{1}H NMR (600Hz) and ^{13}C NMR(151Hz) of the isolated products.

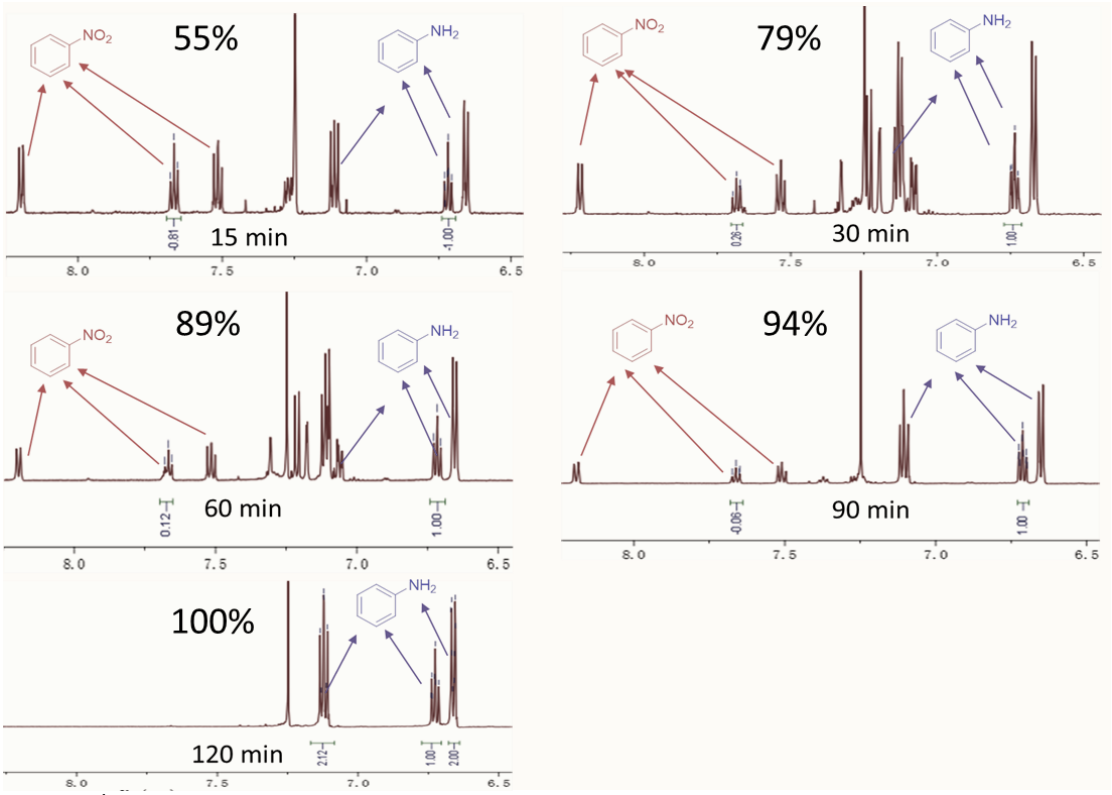

Fig. S15 ^{1}H NMR spectra for hydrazine reduction of nitrobenzene to aniline catalysed by **2** at different reaction time. reaction conditions: **2**, 3 mol%, $PhNO_2$, 10 µL, 0.097 mmol, $N_2H_4{\cdot}H_2O$, 20 µL, 0.3 mmol, EtOH, 2 mL, 80°C.

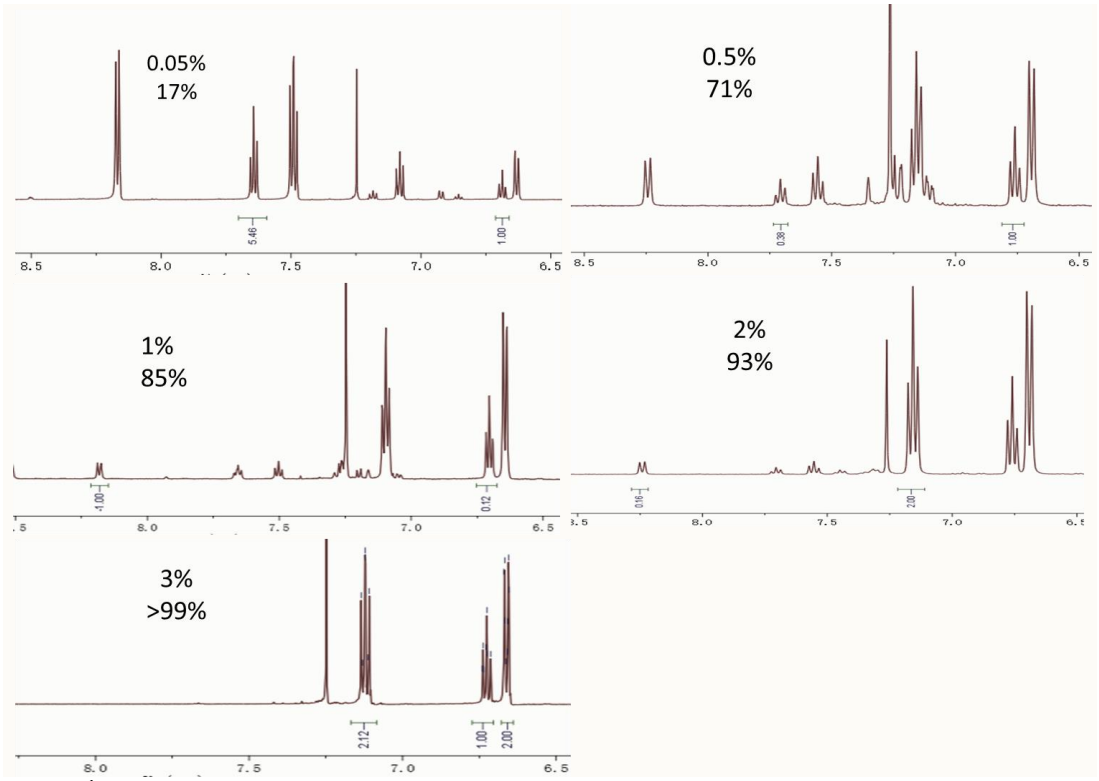

Fig. S16. ^{1}H NMR spectra of products for **2** (0.05-3 mol%) to catalyse hydrazine hydrogenation of nitrobenzene to aniline. reaction conditions: $PhNO_2$, 10 µL, 0.097 mmol, $N_2H_4{\cdot}H_2O$, 20 µL, 0.3 mmol, EtOH, 2 mL, 2h, 80°C.

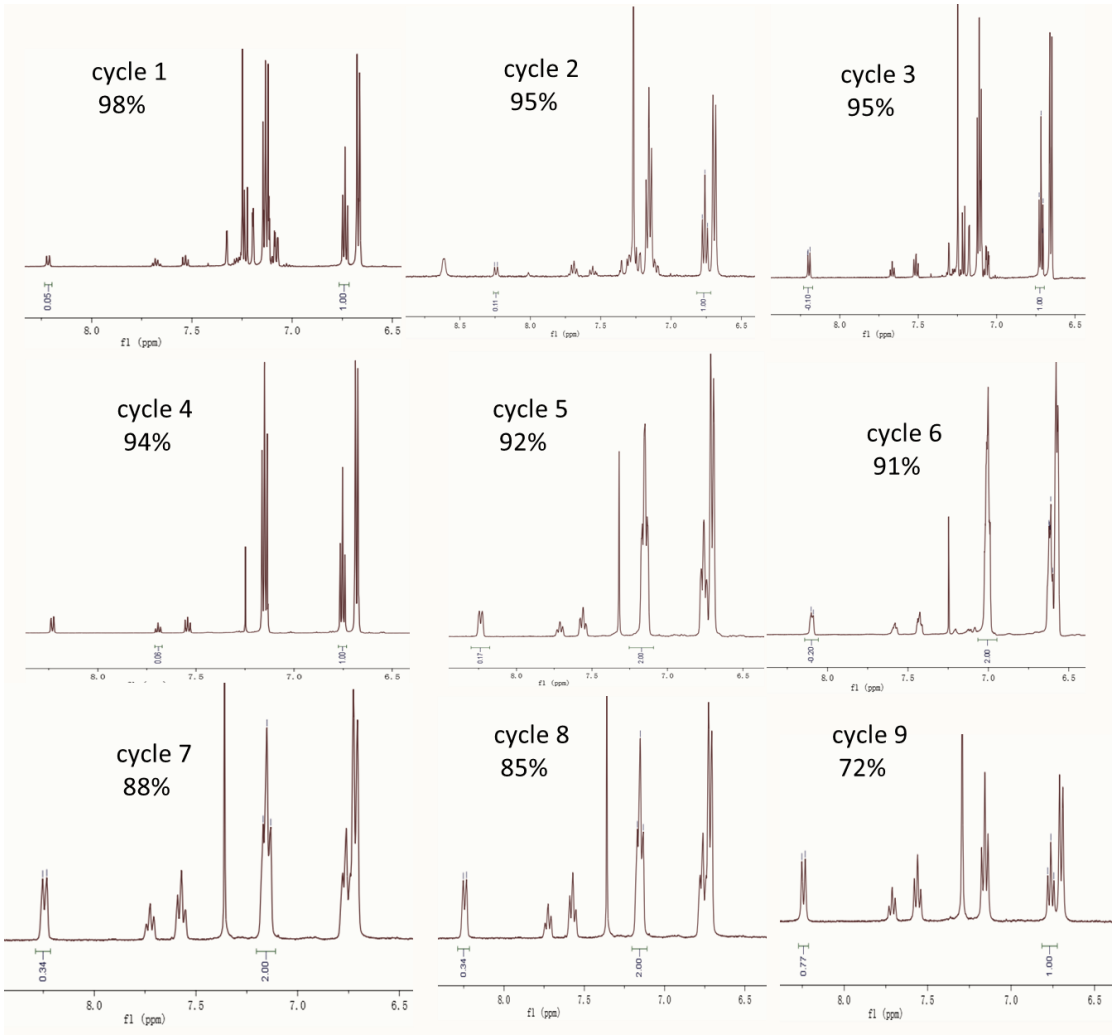

Fig. S17. ^{1}H NMR spectra of products in cycles **1**-**9** for **2** to catalyse hydrazine reduction of nitrobenzene to aniline. catalysis conditions: **2**, 3 mol%, $PhNO_2$, 10 µL, 0.097 mmol, $N_2H_4{\cdot}H_2O$, 20 µL, 0.3 mmol, EtOH, 2 mL, 80°C.

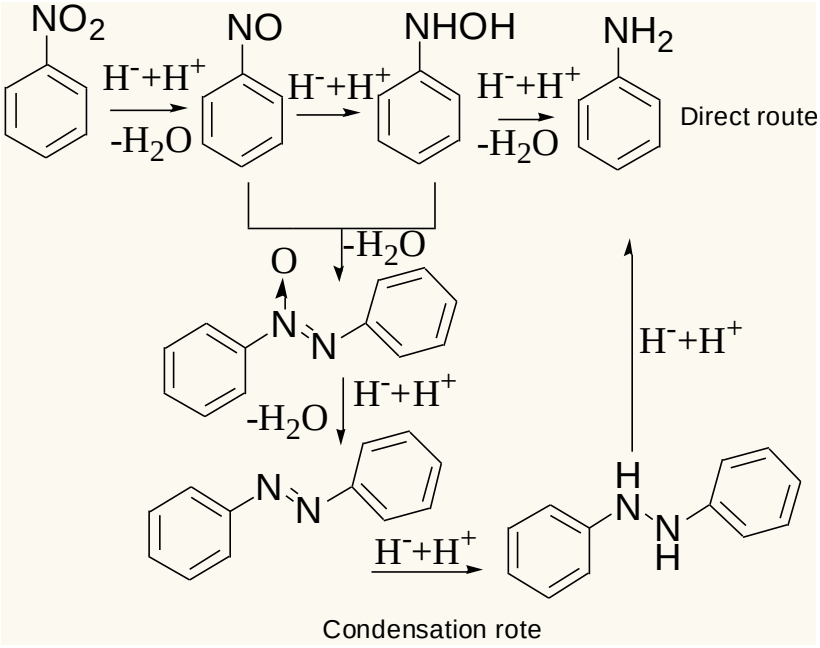

Scheme S1. Direct and condensation route of the nitrobenzene reduction to aniline.

6. Tables

Table **S1** Bond valance sum (BVS) calculation of **2** and **3**.[a]

V1 4.252	V2 4.347	V3 4.528	Mo1 4.315	Mo2 5.229	Mo3 5.560
Mo4 6.198	Mo5 6.129	Mo6 5.910	O1 2.289	O2 1.795	O3 0.278/2.598
O4 2.003	O5 1.926/1.155x2	O6 1.759	O7 2.088	O8 1.834	O9 1.970
O10 2.178	O11 2.058	O12 1.934	O13 2.163	O14 1.827	O15 2.288
O16 2.048	O17 1.939	O18 1.862	O19 2.097	O20 1.1981	
Ge1 4.636	Ge2 3.499	Ge3 4.754	Mo1 5.948	Mo2 4.930	Mo3 5.494
Mo4 4.458	Mo5 6.006	Mo6 6.478	Mo7 5.981	O1 1.757/0.281	O2 2.035
O3 1.927	O4 1.839	O5 1.750	O6 1.778	O7 2.451	O8 1.874
O9 1.988	O10 2.621/1.101x2		O11 1.918	O12 2.041	O13 2.246
O14 2.214	O15 2.113	O16 1.987	O17 2.236	O18 0.454	O19 1.235
O20 1.1981					

[a]Oxygen atoms with the BVS values below 1.2 are assigned as OH^- or H_2O marked in red.